2020

Quantifying the Effect of Uncertainty in the Gas Spot Price on Power System Dispatch Costs with Estimated Correlated Uncertainties

Dan Hu, *Iowa State University*
Sarah M. Ryan, *Iowa State University*

Noname manuscript No.
(will be inserted by the editor)

Quantifying the Effect of Uncertainty in the Gas Spot Price on Power System Dispatch Costs with Estimated Correlated Uncertainties

Dan Hu · Sarah M. Ryan

the date of receipt and acceptance should be inserted later

Abstract Electricity generation increasingly relies on natural gas for fuel. The competing demands for gas by other users who may have higher priority, the lack of coordination between gas and electricity markets, and extreme weather events all pose risks to systems with high dependence on gas. When the gas supply on which generators have planned is limited, operators may dispatch more costly units and generators may switch to alternative fuels or procure gas at high spot prices. All these efforts to avoid load-shedding result in higher electricity costs. To assess this economic risk we approximate the distribution of the daily operational cost to satisfy demand for electricity by conducting simulations of dispatch. Input parameters are sampled from a temporal and weather conditional joint distribution of daily electric load and spot price of gas. To isolate the impact of uncertainty in the gas price, we generate a benchmark distribution of the dispatch cost by fixing the gas price at its expectation while sampling from the marginal distribution for load, and compare the distribution generated from uncertainty in both the gas price and the load against this benchmark. The risk is quantified by alternatively computing the distance between dispatch cost distributions or by the difference between the values of a risk measure applied to each distribution. In a numerical case study we demonstrate how such risk quantification can be used to evaluate alternative risk-mitigation strategies at the system level.

Keywords Economic dispatch · natural gas · bivariate normal distribution · Wasserstein distance · conditional value-at-risk

1 Introduction

Due to the retirements of coal-fired and nuclear generators, the development of highly efficient gas-fired generators, the increase of natural gas supply with a relatively stable gas price over the last decade, and potential emission regulations, natural gas and renewable energy sources have taken a rapidly increasing share of electricity production. Natural gas experiences a more competitive market than other fossil fuels because of its fast procurement and low price. In competitive US electricity markets, gas-fired generators often procure gas in low-cost interruptible contracts and therefore receive lower priority for delivery than gas users with firm contracts. High demand of natural gas by the high-priority customers, which consist of residential, industrial and commercial entities, may cause gas generators to pay high spot prices to avoid outages, as was the experience in the eastern US during early January 2018; the 2013-14 Polar Vortices [24]; and earlier severe-weather events in Texas, New England, and Colorado [23]. Increased reliance on natural gas not only decreases operational cost and environmental pollution but also increases the fuel risk in the power system. Short-term dispatch decisions by the power system operator determine the cost of serving realized electric demand under increasingly constrained gas supply and uncertain spot prices. For the longer term, understanding the risk imposed by dependence on interruptible contracts and exposure to the volatile spot market can help generators and system operators to evaluate potential investments to mitigate the risks.

Our goal in this paper is to present approaches for quantifying the risks imposed by limited natural gas availability and price uncertainty in terms of the probability distribution of daily dispatch cost

Department of Industrial and Manufacturing Systems Engineering, Iowa State University,
Ames, IA 50011-2164 USA.
E-mail: danhu@iastate.edu, smryan@iastate.edu

based on the joint distribution of load and gas spot prices. We generate discrete scenarios for natural gas price jointly with electric load. The impact of uncertainty in natural gas availability is assessed through sensitivity analysis. An electricity system operator can use the quantification methods to evaluate alternative risk-mitigation strategies according to the tradeoff between investment cost and risk reduction.

Previous research has investigated various aspects of the effect of gas system uncertainties on the power system. For evaluating bidding strategies and efficiencies of an integrated gas-fired unit and power-to-gas conversion facility, the financial risk introduced by the uncertain price gap between electricity and natural gas was assessed according to the conditional value at risk (CVaR) [16]. The effect of gas supply uncertainty and gas price variability on unit commitment has been investigated through stochastic programming with a small number of discrete scenarios [27]. However, both [16] and [27] consider only a single natural gas price parameter. In fact, the current gas-fired generators acquire gas from both contracts and the spot market at different prices. While the contracted natural gas price is fixed, that from the spot market has high uncertainty. In addition, the scenarios in the literature are frequently generated without any validation using actual data. Some papers discuss methodologies to assess the forecast uncertainty associated with gas prices; for example, based on weekly data [13]. At the same time, substantial research has been aimed at generating point or probabilistic forecasts of the electric load [7]. The gas spot price is highly correlated with electric load, especially in severe cold weather. But few studies have investigated their joint distribution. To our knowledge, no previous work has addressed the dispatch cost risk resulting from these uncertainties or their influence on the selection of a risk-mitigation strategy.

In this paper, from the viewpoint of an independent system operator (ISO), we propose a dispatch model incorporating the gas availability from both contracts and the spot market. Extending the work in [10], we estimate a joint distribution of daily electric load and gas spot price for use as input to the probabilistic simulation of the dispatch. The objective of this research is to quantify the effect of uncertainties in the availability of contracted natural gas as well as its price in the spot market on the economic dispatch cost. We compare the dispatch cost distributions obtained with and without uncertainty in the spot price for various levels of available contracted gas with the same marginal distribution for electric load. The contributions of this paper are summarized as follows:

- Formulate an economic dispatch model considering gas availability and prices from both the spot market and contracts.
- Generate the joint distribution functions of temporal and weather conditional daily electric load and natural gas spot price by transformation to a bivariate normal distribution.
- To quantify the effect of uncertain natural gas spot price on the dispatch cost, apply the Wasserstein distance metric and a CVaR metric to characterize the difference between the cost distribution functions generated from the two simulations where one simulation uses a point estimate for gas spot price and the other one uses the spot price distribution.
- Demonstrate how to employ the uncertainty quantification to inform choices among alternative risk-mitigation strategies; namely, dual fuel capability conversion and the addition of gas storage facility in a case study.

In the remainder of this paper, the economic dispatch model is formulated in Section 2. In Section 3, we describe how to estimate the joint distribution functions for the daily electric load and the daily gas spot price for different weather conditions and seasons. Section 4 describes the detailed steps of quantifying the effect of uncertain natural gas spot price on dispatch cost. Section 5 revises the dispatch cost model of Section 2 according to alternative risk-mitigation strategies. Case studies and numerical results are shown in Section 6, and finally Section 7 concludes.

2 Economic Dispatch Model (ED) with Natural Gas Availability Constraints

We formulate a linear programming (LP) model of the daily economic dispatch problem with hourly time steps considering gas price and availability from both contracts and the spot market. To focus on the risk imposed by reliance on interruptible contracts, we assume all gas-fired generators choose such contracts for fuel delivery. First we introduce the following notation:

Sets

$\mathcal{J}$	Gas nodes, indexed by j
$\mathcal{J}'(j)$	Gas nodes connected to j by passive pipelines from j, indexed by j'
$\mathcal{J}''(j)$	Gas nodes connected to j by passive pipelines to j, indexed by j''
$\Lambda(j)$	Gas wells in node j, indexed by λ; $\Lambda = \bigcup_{j\in\mathcal{J}} \Lambda(j)$ is the set of all gas wells
$\Psi(j)$	Storage facilities in node j, indexed by ψ; $\Psi = \bigcup_{j\in\mathcal{J}} \Psi(j)$ is the set of all storage facilities
$\Psi'(j)$	Added storage facilities in node j, indexed by ψ; $\Psi' = \bigcup_{j\in\mathcal{J}} \Psi'(j)$ is the set of all added storage facilities
$\mathcal{I}$	Electricity nodes, indexed by i
$\mathcal{I}'(i)$	Electricity nodes connected to i by a transmission line from i, indexed by i'
$\mathcal{I}''(i)$	Electricity nodes connected to i by a transmission line to i, indexed by i''
$\mathcal{G}(i,j)$	Gas-fired generators at power node i and gas node j, indexed by g; $\mathcal{G} = \bigcup_{i\in\mathcal{I},j\in\mathcal{J}} \mathcal{G}(i,j)$ is the set of all gas-fired generators
$\mathcal{G}'(i,j)$	Gas-fired generators converted to dual fuel units at power node i and gas node j, indexed by g'; $\mathcal{G}'(i,j) \in \mathcal{G}(i,j)$; $\mathcal{G}' = \bigcup_{i\in\mathcal{I},j\in\mathcal{J}} \mathcal{G}'(i,j)$ is the set of all gas-fired generators converted to dual fuel units
$\mathcal{N}(i)$	Conventional non-gas-fired generators at node i, indexed by n; $\mathcal{N} = \bigcup_{i\in\mathcal{I}} \mathcal{N}(i)$ is the set of all non-gas-fired generators
$\mathcal{K}$	Set of all gas-fired and non-gas-fired generators, indexed by k; $\mathcal{K} = \mathcal{G} \cup \mathcal{N}$
$\mathcal{T}$	Hours from 1 to $\lvert\mathcal{T}\rvert$, indexed by t

Fixed Parameters

$u_{g,t}, u_{n,t}, u_{k,t}$	Unit commitment indicator: equals 1 if unit is online in hour t and 0 otherwise
$v^u_{g,t}, v^u_{n,t}, v^u_{m,t}$	Unit start-up indicator: equals 1 if the unit is started up in hour t and 0 otherwise
$v^d_{g,t}, v^d_{n,t}, v^d_{m,t}$	Unit shut-down indicator: equals 1 if the unit is shut down in hour t and 0 otherwise
λ^C_g	Gas price from contract [\$/kcf]
λ^Λ_λ	Gas price of the storage outflow [\$/kcf]
$\overline{L}_\psi, \underline{L}_\psi$	Maximum and minimum storage level [kcf]
$\Delta\overline{L}_\psi$	Increased storage capacity [kcf]
$\overline{q}_\psi$	Max net flow (outflow minus inflow) [kcf]
ϕ_g	Efficiency of gas generator [kcf/MWh]
$\phi^{oil}_{g'}$	Cost of using oil as dual fuel [\$/MWh]
C^{prod}_n	Power production cost [\$/MWh]
$\Gamma^-_\beta, \Gamma^+_\beta$	Unserved/excess electric penalty [\$/MWh]
$\Gamma^-_\alpha, \Gamma^+_\alpha$	Unserved/excess gas penalty [\$/kcf]
$\overline{P}_g, \underline{P}_g, \overline{P}_n, \underline{P}_n, \overline{P}_k, \underline{P}_k$	Max/min electricity generation [MWh]
$\overline{F}_{i,i'}$	Max line flow from i to i' [MWh]
$x_{i,i'}$	Transmission line impedance from i to i' [pu]
$\overline{G}_{j,t}$	Nominal available gas from gas contract for the power system as planned in day-ahead unit con

Uncertain Parameters

$D_{i,t}$	Electric load [MWh]
Λ^M	Gas price in the spot market [\$/kcf]

Nonnegative Decision Variables

$\alpha^-_{j,t}$,$\alpha^+_{j,t}$	Unserved/excess gas [kcf]
$l_{\psi,t}$	Storage level [kcf]
$p_{g,t}, p_{n,t}, p_{k,t}$	Electricity production [MWh]
$\beta^-_{i,t}$,$\beta^+_{i,t}$	Unserved/excess electricity [MWh]
$q^{out}_{\psi,t}, q^{in}_{\psi,t}$	Out/in-flow of storage facility [kcf/h]
$m_{j,t}$	Gas from spot market for the power system [kcf]
$\eta^C_{g,t}$	Consumed gas from pipeline contract [kcf]
$\eta^M_{g,t}$	Consumed gas from spot market [kcf]

Unrestricted Decision Variables

$\theta_{i,t}$	Phase angle [rad]
$f_{i,i',t}$	Line flow from i to i' [MWh]

The economic dispatch model including constraints on contracted gas availability and prices from both contract and the spot market is formulated as follows:

$$\min \sum_{t\in\mathcal{T}} \Bigg\{ \sum_{g\in\mathcal{G}} \lambda_g^C \eta_{g,t}^C + \sum_{j\in\mathcal{J}} \Lambda^M m_{j,t} + \sum_{n\in\mathcal{N}} C_n^{prod} p_{n,t} + \sum_{\psi\in\Psi} \lambda_{\psi,t}^{\Psi} q_{\psi,t}^{out} + \sum_{i\in\mathcal{I}} \left(\Gamma_\beta^+ \beta_{i,t}^+ + \Gamma_\beta^- \beta_{i,t}^- \right) + \sum_{j\in\mathcal{J}} \left(\Gamma_\alpha^+ \alpha_{j,t}^+ + \Gamma_\alpha^- \alpha_{j,t}^- \right) \Bigg\} \tag{1}$$

s.t.

$$\sum_{j\in\mathcal{J}} \sum_{g\in\mathcal{G}(i,j)} p_{g,t} + \sum_{n\in\mathcal{N}(i)} p_{n,t} + \sum_{i''\in\mathcal{I}''(i)} f_{i'',i,t} + \beta_{i,t}^- = D_{i,t} + \sum_{i'\in\mathcal{I}'(i)} f_{i,i',t} + \beta_{i,t}^+, \quad \forall i,t \tag{2}$$

$$p_{k,t} \geq \underline{p}_k \left(u_{k,t} - v_{k,t}^u \right), \quad \forall k \in \mathcal{K}, t \tag{3}$$

$$p_{k,t} \leq \overline{p}_k \left(u_{k,t} - v_{k,t}^u \right) + \underline{p}_k \left(v_{k,t}^d + v_{k,t}^u \right), \quad \forall k \in \mathcal{K}, t \tag{4}$$

$$f_{i,i',t} = \frac{\theta_{i,t} - \theta_{i',t}}{x_{i,i'}}, \quad \forall i' \in \mathcal{I}'(i), i, t \tag{5}$$

$$-\overline{F}_{i,i'} \leq f_{i,i',t} \leq \overline{F}_{i,i'}, \quad \forall i' \in \mathcal{I}'(i), i, t \tag{6}$$

$$\phi_g p_{g,t} = \eta_{g,t}^C + \eta_{g,t}^M + \eta_{g,t}^{out}, \quad \forall g, t \tag{7}$$

$$\sum_{i\in\mathcal{I}} \sum_{g\in\mathcal{G}(i,j)} \eta_{g,t}^C \leq \rho \overline{G}_{j,t}, \quad \forall j, t \tag{8}$$

$$\sum_{i\in\mathcal{I}} \sum_{g\in\mathcal{G}(i,j)} \phi_g p_{g,t} + \alpha_{j,t}^+ \leq \rho \overline{G}_{j,t} + m_{j,t} + \sum_{\psi\in\Psi(j)} \left(q_{\psi,t}^{out} - q_{\psi,t}^{in} \right) + \alpha_{j,t}^-, \quad \forall j, t \tag{9}$$

$$\underline{L}_\psi \leq l_{\psi,t} \leq \overline{L}_\psi, \quad \forall \psi, t \tag{10}$$

$$-\overline{q}_\psi \leq \left(q_{\psi,t}^{out} - q_{\psi,t}^{in} \right) \leq \overline{q}_\psi, \quad \forall \psi, t \tag{11}$$

$$l_{\psi,t} = l_{\psi,t-1} - q_{\psi,t}^{out} + q_{\psi,t}^{in}, \quad \forall \psi, t \tag{12}$$

The daily economic dispatch (ED) problem finds production quantities for the committed thermal units for each hour that minimize the total cost including the production cost and penalties for energy imbalances while satisfying the electric load, transmission and other operational constraints. The objective (1) is to minimize the total daily dispatch cost including the fuel cost from contracts and the spot market for gas-fired generators, the production cost of the non-gas generators, the net cost of gas flows from storage and the penalties on non-served or excess electricity and gas demands. Constraints (2) enforce the power balance at each electricity node for each hour. Constraints (3)–(4) limit the maximum and minimum production by each generator based on its commitment status in each hour. Constraints (5)–(6) compute and limit the flows through transmission lines according to a linear DC approximation. Constraints (7) compute the gas consumption, which is composed of gas from contracts, spot market and storage facilities. Constraints (8) dictate that the total gas quantity consumed by the gas-fired generators does not exceed the current available gas quantity from the contracts. To assess the effect of uncertainty in the gas availability on the dispatch cost, a contracted gas availability factor, ρ, and a nominal available gas quantity from gas contracts for the power system, $\overline{G}_{j,t}$, are respectively defined as parameters. The latter is determined along with the unit commitment status parameter in a prior optimization. Thus, $\rho\overline{G}_{j,t}$ represents various levels of contracted gas availability. Any $\rho < 1$ indicates that less gas than desired is available, and thus the committed gas-fired generators cannot obtain enough gas from contracts and must acquire gas from the spot market. Meanwhile, some non-gas-fired generators might have to be dispatched at higher levels. Any $\rho > 1$ indicates a surplus, in which case the gas-fired generators have more flexibility of obtaining gas from the spot market if the spot price is low or as contracted from the pipeline if the spot price is high. Constraints (9) express the gas balance for each hour at each gas node where a linear function is applied to describe the input-output curve [14]. Constraints (10)–(11) define the upper and lower limits on the storage levels and flow rates of each gas storage facility. Constraints (12) connect storage levels of consecutive hours.

3 Uncertainty Identification

We view the electric load and natural gas spot price as the two uncertain quantities in the economic dispatch model formulated in Section 2. Given a specific realization of electric load and spot price, we can obtain the corresponding dispatch cost. Thus, it is crucial to estimate the joint distribution of daily electric load and natural gas spot price. Historical electric load and natural gas spot price data, along with the corresponding weather data, can be obtained from system operator and local natural gas hub records. Our goal in this section is to use the available data to generate discrete realizations that can be used individually as input to the ED model formulated in Section 2. The simulated dispatch cost distribution can be constructed from the outputs of multiple simulation replications.

To improve the accuracy of estimating the correlation and generating scenarios, similar weather days in the same season are clustered using the K-means method. The details of K-means method and definition of a distortion metric which helps to decide the number of clusters can be found in [22]. Within each cluster, a joint distribution of electric load and gas price is generated. Among parametric approaches to fitting continuous bivariate observations, the bivariate normal distribution is frequently used [2]. The Box-Cox transformation is the most common approach to transforming observations to achieve normality [3]. A nonnegative observation $y = \left(y_1, ..., y_Z\right)$ of dimension Z can be transformed to $y^{(\tau)} = \left(y_1^{(\tau_1)}, ..., y_Z^{(\tau_Z)}\right)$ by applying Eq. (13), where $\tau = (\tau_1, ..., \tau_Z)$ is a vector with the same dimension as the observation. Based on the assumption that $y^{(\tau)}$ follows a bivariate normal distribution, the maximum-likelihood estimate of τ can be obtained according to the detailed steps described in [3].

$$y_z^{(\tau_z)} = \begin{cases} \dfrac{y_z^{\tau_z} - 1}{\tau_z} & (\tau_z \neq 0) \\ \log y_z & (\tau_z = 0) \end{cases}, \forall z \in \{1, ..., Z\} \tag{13}$$

One of the several tests for bivariate normality such as Mardias, Henze-Zirklers and Roystons normality tests as well as the graphical approach of constructing a chi-square quantile-quantile (Q-Q) plot [15] may then be applied to test goodness of fit. The best number of clusters is chosen considering distortion [22] and the results of goodness of fit tests within each cluster.

In our application, as the generated bivariate normal distribution is continuous, to obtain a tractable number of input scenarios for the dispatch simulation in each cluster, we first generate a large sample of realized (gas price, electricity load) pairs from the fitted distribution for that cluster. Much research has been done on scenario generation and reduction as well as continuous distribution discretization. Because this is not the focus of this research, we simply construct a bivariate histogram of the randomly sampled observations. The center of each bin of the histogram is adopted as one scenario and the relative frequency for that bin is taken as the scenario probability. More accurate and tractable scenario generation and reduction methods can be found in [5, 22].

4 Quantification Metrics

Given the model presented in Section 2 and the discrete scenarios generated by the methods in Section 3, this section presents methodologies to quantify the effect of natural gas spot price uncertainty on the economic dispatch cost uncertainty. We review and apply the Wasserstein distance measure and the CVaR risk measure in Sections 4.1 and 4.2, respectively. The detailed quantification steps are illustrated in Section 4.3.

4.1 Review of Wasserstein Distance (WD)

The Wasserstein distance was proposed to measure the distance between probability distributions [19]. If $\boldsymbol{H}$ and $\boldsymbol{R}$ are discrete probability distributions having finitely many scenarios ξ_s (with probabilities h_s), $s = 1, ..., S$, and $\tilde{\xi}_{s'}$ (with probabilities $r_{s'}$), $s' = 1, ..., S'$, respectively, we obtain the Wasserstein distance as Eq. (14) where $d(\xi_s, \tilde{\xi}_{s'})$ is the distance between scenario ξ_s in $\boldsymbol{H}$ and $\tilde{\xi}_{s'}$ in $\boldsymbol{R}$ according to some norm.

$$\text{WD} = inf\left\{ \sum_{s=1}^{S} \sum_{s'=1}^{S'} d(\xi_s, \tilde{\xi}_{s'}) y_{s,s'} : \quad y_{s,s'} \geq 0, \quad \sum_{s'=1}^{S'} y_{s,s'} = h_s, \quad \sum_{s=1}^{S} y_{s,s'} = r_{s'} \right\} \tag{14}$$

4.2 Review of Conditional Value at Risk (CVaR)

The CVaR was described in [20] as a coherent risk measure. For a cost probability density function $f_X(x)$ and a confidence level $\gamma \in (0,1)$, which usually is set to be 0.95 or 0.99, value at risk (VaR) and CVaR are defined as follows:

Definition 1 (VaR) The value-at-risk measure for a random variable with cumulative distribution function (cdf) F is defined as:

$$\mathrm{VaR}_\gamma(\mathrm{F}) = inf\{x : \mathrm{F}(x) \geq \gamma\}. \tag{15}$$

Definition 2 (CVaR) The conditional value-at-risk measure is defined as:

$$\mathrm{CVaR}_\gamma(\mathrm{F}) = \frac{1}{1-\gamma}\int_{\mathrm{VaR}_\gamma(\mathrm{F})}^{\infty} x d\mathrm{F}(x). \tag{16}$$

Definition 3 (CVaR for discrete probability distributions) The conditional value-at-risk measure for discrete probability distribution F such that $f_X(x) = \Pr(X = x) = \Pr(\{\omega \in \Omega : X(\omega) = x\})$ is defined as:

$$\mathrm{CVaR}_\gamma(\mathrm{F}) = \frac{1}{1-\gamma}\sum_{\omega\in\Omega}\Big\{\Pr(\omega)\Big(\mathrm{VaR}_\gamma(\mathrm{F}) + [X(\omega) - \mathrm{VaR}_\gamma(\mathrm{F})]^+\Big)\Big\}. \tag{17}$$

Algorithm 1 is a procedure to compute CVaR according to Eq. (17).

Algorithm 1: CVaR Evaluation for a Discrete Probability Distribution

Input: Discrete probability distribution F, sorted mass points $x^1 \leq x^2 \leq ... \leq x^N$ and the corresponding probabilities $p^1, p^2, ..., p^N$, confidence level γ

Output: The CVaR of distribution F : $\mathrm{CVaR}_\gamma(\mathrm{F})$

```
i = 1
while Σ_{n=1}^{i} p^n < γ do
    i = i + 1
i* = i, VaR_γ(F) = x^{i*}
CVaR_γ(F) = 1 / (Σ_{n=i*}^{N} p^n) Σ_{n=i*}^{N} (x^n p^n)
Return CVaR_γ(F)
```

4.3 Quantifying Steps

We use the WD and CVaR metrics to compare the cost distributions resulting from the economic dispatch with price estimate (ED-PE) simulation, where the load uncertainty is considered but the price uncertainty is not, and the economic dispatch with price distribution (ED-PD) simulation, where both uncertainties are included, as illustrated in Fig. 1. The method can be applied to each segment of each season and is summarized as follows:

Step 1: Obtain input parameter values, including unit commitment/start-up/shut-down indicators $(u_{k,t}, u^u_{k,t}, v^d_{k,t})$ and available gas from contracts $(\overline{G}_{j,t})$ by solving the day-ahead unit commitment (UC) problem. The detailed formulation of the UC model can be found in [11]. The UC model includes a reserve requirement and natural gas network constraints of pipelines as well as storage facilities using the 24-hour electric load point estimates and contracted gas only. Set the optimal UC decisions and hourly schedule of the gas network as the input parameters of the ED model.

Step 2: **(ED-PE simulation)** Solve the ED model for each scenario from the electric load probability distribution $P_{i,t}(D)$ and the **point estimate of the gas spot price**. Construct the corresponding discrete dispatch cost probability distribution $\boldsymbol{H}$ having finitely many scenarios ξ_s (with probabilities h_s), $s = 1, ..., S$, where ξ_s denotes optimal cost of scenario s for the ED-PE simulation.

Step 3: **(ED-PD simulation)** Solve the ED model for each scenario of the joint probability distribution of the electric load and the gas spot price. Construct the corresponding discrete dispatch cost probability distribution $\boldsymbol{R}$ having finitely many scenarios $\tilde{\xi}_{s'}$ (with probabilities $r_{s'}$), $s = 1, ..., S'$, where $\tilde{\xi}_{s'}$ denotes optimal cost of scenario s' for the ED-PD simulation.

Step 4: Compare the two dispatch cost probability distribution, $\boldsymbol{H}$ and $\boldsymbol{R}$. Calculate the Wasserstein distance (WD) as the optimal cost of model (14) [9], where $d(\xi_s, \tilde{\xi}_{s'})$ and $y_{s,s'}$ are the distance and flow between the costs of scenarios s and s', respectively. Calculate CVaR_γ of $\boldsymbol{H}$ and $\boldsymbol{R}$ using Algorithm 1. Then the CVaR difference between the ED-PD simulation and the ED-PE simulation can be assessed as $\Delta\text{CVaR}_\gamma = \text{CVaR}_\gamma(\boldsymbol{R}) - \text{CVaR}_\gamma(\boldsymbol{H})$.

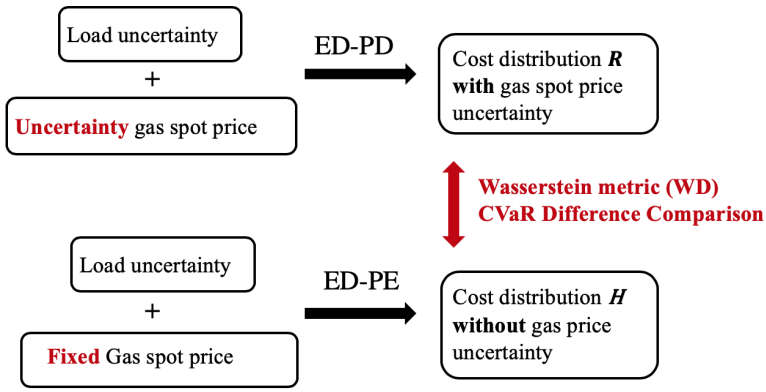

Fig. 1: Illustration of procedure to quantify impact of gas price uncertainty

5 Applying WD and CVaR Metrics to Assess Risk-Mitigation Strategies Selection

The previous sections discuss how to assess the WD and CVaR metrics to quantify the effect of gas spot price uncertainty on the risk of dispatch cost for the daily short-term operation. To reduce this risk, the ISO can coordinate or suggest to generator owners some risk-mitigation strategies, such as converting natural gas fueled units into dual-fuel units and building new gas storage facilities. Both of these strategies potentially are able to reduce risk but also will result in conversion and installation costs. In this section we present revisions to the daily short-term dispatch model to reflect the adoption of either risk-mitigation strategy. Using these revised models, modified values of the WD and CVaR metrics can be assessed by the methods described in Section 4.3.

5.1 Strategy 1: Dual Fuel Conversion

Adding dual fuel, such as fuel oil, capability is a useful strategy to mitigate the effect of natural gas price volatility. Conversion of natural gas fueled generators to be able to operate on an alternative fuel requires building fuel storage tanks, which results in a one-time conversion cost. For the operation of a dual fuel generator, it takes some time, ranging from 4 to 72 hours, to switch between fuels. Here we assume that within one day, a converted generator can only use one kind of fuel. The effect of having dual fuel capability on the economic dispatch model is to include fuel-switching decisions based on the cost minimization shown in Eq. (18), where ζ_g is the daily production cost of a converted generator, g.

$$\zeta_g = inf\left\{\sum_{t\in\mathcal{T}}\left(\lambda_g^C\eta_{g,t}^C + \Lambda^M\eta_{g,t}^M + \lambda_\psi^\Psi\eta_{g,t}^{out}\right), \sum_{t\in\mathcal{T}}\phi_g^{oil}p_{g,t}\right\}, \forall g \in \mathcal{G}'(i,j), \psi \in \Psi(j) \tag{18}$$

The gas balance constraint (9) becomes (19). The first expression of the left hand side of (9) is divided into two parts in (19) where the first part is the gas consumption by the non-converted gas generators and the second part represents the gas consumption by the converted gas generators. Here for each converted generator, we use $b_g(\eta^C_{g,t}+\eta^M_{g,t}+\eta^{out}_{g,t}) = b_g\phi_g p_{g,t}$ to indicate the gas consumption, where b_g is a binary variable indicating whether natural gas results in a smaller cost, compared with the alternative fuel. While producing a fixed amount of power, $b_g = 1$ if the gas fuel cost is lower and $b_g = 0$ otherwise, as illustrated in Eq. (20a)–(20b).

$$\sum_{i\in\mathcal{I}}\sum_{g\in\mathcal{G}(i,j)\setminus\mathcal{G}'(i,j)}\phi_g p_{g,t}+\sum_{i\in\mathcal{I}}\sum_{g\in\mathcal{G}'(i,j)} b_g\phi_g p_{g,t}+\alpha^+_{j,t}\le\rho\overline{G}_{j,t}+m_{j,t}+\sum_{\psi\in\Psi(j)}\left(q^{out}_{\psi,t}-q^{in}_{\psi,t}\right)+\alpha^-_{j,t},\quad\forall j,t \tag{19}$$

where

$$b_g = 1, \text{if}\quad \sum_{t\in\mathcal{T}}\left(\lambda^C_g\eta^C_{g,t}+\Lambda^M\eta^M_{g,t}+\lambda^\Psi_\psi\eta^{out}_{g,t}\right)\le\sum_{t\in\mathcal{T}}\phi^{oil}_g p_{g,t}, \forall g\in\mathcal{G}'(i,j),\psi\in\Psi(j) \tag{20a}$$

$$b_g = 0, \text{if}\quad \sum_{t\in\mathcal{T}}\left(\lambda^C_g\eta^C_{g,t}+\Lambda^M\eta^M_{g,t}+\lambda^\Psi_\psi\eta^{out}_{g,t}\right)>\sum_{t\in\mathcal{T}}\phi^{oil}_g p_{g,t}, \forall g\in\mathcal{G}'(i,j),\psi\in\Psi(j). \tag{20b}$$

Constraints (18)–(20b) are nonlinear and may introduce solutions that are locally but not globally optimal. Thus we transform them into mixed integer linear constraints via the disjunctive method. Constraints (18) can be linearized as (21a)–(21e), where b_g can be assessed and M_1 is a big number. Constraints (22) are added because now we must determine the exact amount of gas the converted generator consumes from the storage facility which influences the objective function. Constraints (19) are linearized as Eq. (23a)–(23e) where another big number M_2 is used and a new variable $z_{g,t} \equiv b_g(\eta^C_{g,t}+\eta^M_{g,t}+\eta^{out}_{g,t}) = b_g\phi_g p_{g,t}$, is introduced.

$$\zeta_g\le\sum_{t\in\mathcal{T}}(\lambda^C_g\eta^C_{g,t}+\Lambda^M\eta^M_{g,t}+\lambda^\Psi_\psi\eta^{out}_{g,t}), \forall g\in\mathcal{G}'(i,j),\psi\in\Psi(j) \tag{21a}$$

$$\zeta_g\le\sum_{t\in\mathcal{T}}\phi^{oil}_g p_{g,t}, \forall g\in\mathcal{G}'(i,j),\psi\in\Psi(j) \tag{21b}$$

$$\zeta_g\ge\sum_{t\in\mathcal{T}}(\lambda^C_g\eta^C_{g,t}+\Lambda^M\eta^M_{g,t}+\lambda^\Psi_\psi\eta^{out}_{g,t})-M_1(1-b_g), \forall g\in\mathcal{G}'(i,j),\psi\in\Psi(j) \tag{21c}$$

$$\zeta_g\ge\sum_{t\in\mathcal{T}}\phi^{oil}_g p_{g,t}-M_1 b_g, \forall g\in\mathcal{G}'(i,j),\psi\in\Psi(j) \tag{21d}$$

$$b_g \quad \text{is binary}, \forall g\in\mathcal{G}'(i,j) \tag{21e}$$

$$\sum_{i\in\mathcal{I}}\sum_{g\in\mathcal{G}(i,j)}\eta^{out}_{g,t}=\sum_{\psi\in\Psi(j)}q^{out}_{\psi,t}, \forall t \tag{22}$$

$$\sum_{i\in\mathcal{I}}\sum_{g\in\mathcal{G}(i,j)\setminus\mathcal{G}'(i,j)}\phi_g p_{g,t}+\sum_{i\in\mathcal{I}}\sum_{g\in\mathcal{G}'(i,j)} z_{g,t}+\alpha^+_{j,t}\le\rho\overline{G}_{j,t}+m_{j,t}+\sum_{\psi\in\Psi(j)}\left(q^{out}_{\psi,t}-q^{in}_{\psi,t}\right)+\alpha^-_{j,t},\quad\forall j,t \tag{23a}$$

$$z_{g,t}\le M_2 b_g, \forall g\in\mathcal{G}'(i,j),t \tag{23b}$$

$$z_{g,t}\le\phi_g p_{g,t}, \forall g\in\mathcal{G}'(i,j),t \tag{23c}$$

$$z_{g,t}\ge\phi_g p_{g,t}-M_2(1-b_g), \forall g\in\mathcal{G}'(i,j),t \tag{23d}$$

$$z_{g,t}\ge 0, \forall g\in\mathcal{G}'(i,j),t \tag{23e}$$

Finally, the revised ED model with dual fuel conversion strategy is formulated as follows. The objective function (24) is revised based on (1). The difference is that the fuel cost is computed separately for the converted generators and non-converted generators. Since all the storage outflow costs are considered in the fourth expression, we must take care with the definition of the first expression. According to the previous discussion, given $b_g = 0$, the alternative fuel is used, and ζ_g in the first expression represents the fuel cost of using the alternative fuel. However, for this converted generator, the storage outflow variable still has some nonnegative values because we are comparing the costs of using alternative fuel and natural gas and choosing the fuel with a cheaper cost. The fourth expression, the total storage outflow cost, includes the storage outflow cost of the converted generator, which is not actually used. So we have to deduct the storage outflow cost from the converted generator when the alternative fuel

is selected. If $b_g = 1$, then natural gas is used, and the first expression represents the total production cost minus the storage outflow cost for the converted generators since all the storage outflow costs are calculated through the fourth expression. The revised dispatch model is:

$$\begin{aligned}\min \sum_{g\in\mathcal{G}'}(\zeta_g - \sum_{t\in\mathcal{T}}\lambda^{\Psi}_{\psi}\eta^{out}_{g,t}) + \sum_{t\in\mathcal{T}}\Bigg\{ \sum_{g\in\mathcal{G}\setminus\mathcal{G}'}\left(\lambda^C_g\eta^C_{g,t} + \Lambda^M\eta^M_{g,t}\right) + \sum_{n\in\mathcal{N}} C^{prod}_n p_{n,t} \\ + \sum_{\psi\in\Psi}\lambda^{\Psi}_{\psi}q^{out}_{\psi,t} + \sum_{i\in\mathcal{I}}\left(\Gamma^+_{\beta}\beta^+_{i,t} + \Gamma^-_{\beta}\beta^-_{i,t}\right) + \sum_{j\in\mathcal{J}}\left(\Gamma^+_{\alpha}\alpha^+_{j,t} + \Gamma^-_{\alpha}\alpha^-_{j,t}\right)\Bigg\}\end{aligned} \tag{24}$$

$$\text{s.t.}(2)-(8),(10)-(12),(21a)-(21e),(22),(23a)-(23e).$$

5.2 Strategy 2: Adding Gas Storage Facilities

Adding gas storage facilities is another strategy to mitigate risk. Here we define $\Psi'(j)$ as the set of added gas storage facilities at gas node j, and the revised ED model is as follows. The only difference between this model and the ED model from Section 2 is that all the expressions involving $\Psi(j)$ and Ψ are replaced with $\Psi(j)\cup\Psi'(j)$ and $\Psi\cup\Psi'$, respectively, to reflect the presence of the additional gas storage facilities.

$$\begin{aligned}\min \sum_{t\in\mathcal{T}}\Bigg\{ \sum_{g\in\mathcal{G}}\lambda^C_g\eta^C_{g,t} + \sum_{j\in\mathcal{J}}\Lambda^M m_{j,t} + \sum_{n\in\mathcal{N}} C^{prod}_n p_{n,t} + \sum_{\psi\in\Psi\cup\Psi'}\lambda^{\Psi}_{\psi,t}q^{out}_{\psi,t} + \sum_{i\in\mathcal{I}}\left(\Gamma^+_{\beta}\beta^+_{i,t} + \Gamma^-_{\beta}\beta^-_{i,t}\right) \\ + \sum_{j\in\mathcal{J}}\left(\Gamma^+_{\alpha}\alpha^+_{j,t} + \Gamma^-_{\alpha}\alpha^-_{j,t}\right)\Bigg\}\end{aligned} \tag{25}$$

s.t.

$$(2)\text{-}(8)$$

$$\sum_{i\in\mathcal{I}}\sum_{g\in\mathcal{G}(i,j)}\phi_g p_{g,t} + \alpha^+_{j,t} \le \rho\overline{G}_{j,t} + m_{j,t} + \sum_{\psi\in\Psi(j)\cup\Psi'(j)}\left(q^{out}_{\psi,t} - q^{in}_{\psi,t}\right) + \alpha^-_{j,t}, \quad \forall j,t \tag{26}$$

$$\underline{L}_{\psi} \le l_{\psi,t} \le \overline{L}_{\psi}, \quad \forall\psi\in\Psi\cup\Psi', t \tag{27}$$

$$-\overline{q}_{\psi} \le \left(q^{out}_{\psi,t} - q^{in}_{\psi,t}\right) \le \overline{q}_{\psi}, \quad \forall\psi\in\Psi\cup\Psi', t \tag{28}$$

$$l_{\psi,t} = l_{\psi,t-1} - q^{out}_{\psi,t} + q^{in}_{\psi,t}, \quad \forall\psi\in\Psi\cup\Psi', t \tag{29}$$

5.3 Comparison of Risk-Mitigation Strategies

The daily cost distributions of each strategy can be obtained using the discrete scenarios generated in Section 3 and quantification method in Section 4 along with the revised ED model in Sections 5.1 and 5.2. A comparison between the quantification measures in the form of the WD and CVaR metrics and the corresponding conversion or installation costs informs the choice of the better strategy. This method can be extended to other risk-mitigation strategies including building new pipelines and signing firm gas transportation contracts.

Now we have two strategies of dual fuel conversion and adding storage facilities. We assume the dual fuel conversion cost is C^D (\$/MW). Suppose one option is to convert a specific natural gas generator with a capacity of $\bar{P}_g$ into a dual fuel generator. If the installation cost of a new storage facility is C^S (\$/kcf) at the same location, then the investment cost of dual fuel conversion could alternatively be used to build a storage facility with a maximum capacity of $\bar{P}_g C^D/C^S$. With the same investment, the strategy that results in a greater reduction of risk as quantified by the WD metric or CVaR difference between the ED-PD result and the ED-PE result is preferred. Use R^1, R^2 to indicate the risk measures for strategy 1 and 2, respectively. Strategy 1 is preferred if $\mathrm{R}^1 < \mathrm{R}^2$ and strategy 2 is preferred otherwise, where $\mathrm{R} \in \left\{\mathrm{WD}, \Delta\mathrm{CVaR}_{\gamma}\right\}$ as defined in the Eqs. (30a)–(30b). Since the risk-mitigation strategies have different results for each segment and each contracted gas availability factor, we assign each segment risk a weight a_c and each contracted gas availability factor case a weight b_{ρ} where $c \in \mathcal{C}$ is a segment index and ρ is the contracted gas availability factor, respectively. Let $\mathrm{R}^1_{c,\rho}, \mathrm{R}^2_{c,\rho}$ indicate the risk measures for

strategies 1 and 2 for segment c and contracted gas availability factor ρ, respectively. Then the composite risk measures are constructed as:

$$\mathrm{R}^1 = \sum_{\rho} \sum_{c \in \mathcal{C}} b_\rho a_c \mathrm{R}^1_{c,\rho}, \tag{30a}$$

and

$$\mathrm{R}^2 = \sum_{\rho} \sum_{c \in \mathcal{C}} b_\rho a_c \mathrm{R}^2_{c,\rho}. \tag{30b}$$

6 Case Study

Currently there are no available large test cases of the coordinated operation of a real natural gas and power system. We provided an extensive literature review of the current available test cases in [21]. But all of them are artificial. The IEEE 24-bus power system with Belgian 20-node natural gas system has been used frequently as a large system tested in previous papers including [26]. We apply our models in a case study of a modified IEEE 24-bus system with a modified Belgian 20-node natural gas system [4]. The cost function is revised according to [18]. The non-served energy penalty cost is set to be \$3500/MWh, as recommended by Midcontinent Independent System Operator [17]. The excess energy penalty cost is set to be \$350/MWh, while the non-served gas and excess gas penalties are set to be \$3500/kcf and \$350/kcf, respectively. The gas price from contracts is set to be \$2.0/kcf and we assume for simplicity that 1 kcf of natural gas can generate 1 MBtu of energy. ISO New England (ISO–NE) provided the electric load and weather data for each of its eight zones including Connecticut (CT), North Central Massachusetts, West Central Massachusetts, Southeast Massachusetts, Maine, New Hampshire, Rhode Island and Vermont. Since CT accounts for the greatest share, about 25% of the electricity assumption of ISO–NE, we apply a case study for CT only. The total for the system is set to be that for CT and is allocated to buses according to the same proportions as in the IEEE 24-bus system load data. The non-electric natural gas demand is set to equal that of the Belgian 20-node natural gas system. The Algonquin Citygate natural gas price for ISO–NE is taken as the gas price for the Belgian 20-node natural gas system. The optimal unit commitment decisions and natural gas network schedules of the day-ahead short-term scheduling model of the combined natural gas and power system with reserves of 3% are fixed to be the initial values of the unit commitment parameters $u_{k,t}, v^u_{k,t}, v^d_{k,t}$ and gas availability from gas contract $\overline{G}_{j,t}$. The linear programs are solved with GAMS/CPLEX 23.4.3 on a Linux workstation (24 CPU, 94GB RAM).

6.1 Uncertainty Identification

As explained in Section 3, we generate discrete scenarios for correlated electric load and natural gas price for each weather information segment. This section describes the sources of historical data for the uncertain parameters and shows the best clustering result. For each segment of each season, the joint distribution of the electric load and the natural gas spot price is generated, where bivariate normal distributions are seen to be valid after data transformation. Lastly, we present the generated discrete scenarios for correlated electric load and gas price.

6.1.1 Data Sources

Hourly electric load data can be obtained from ISO–NE for each year [12]. ISO–NE also provided us with weather data including temperature, dew point and wind speed from 2012–12–31 to 2016–11–07 for each hour of each day. We use Algonquin Citygate natural gas pot price as the reference natural gas spot price index for the ISO–NE area, available from 2014–03–17 to 2017–01–03 [25]. Because the natural gas spot price is recorded daily, we sum the hourly electric load data to find the corresponding daily electric loads. A similar process is followed for the daily average weather information. According to the regression result of [7] and because each season has its own typical electric load pattern, the electric load data are divided into three seasons, spring/fall (April 1–May 14 and September 15–November 30), summer (May 15–September 14) and winter (December 1–March 31). Altogether we had available data of daily weather information (temperature, dew point and wind speed), the daily electric load and the daily natural gas spot price for ISO–NE from 2014-03-17 to 2016–11–07. We display results only for winter in CT because in winter natural gas price intends to have high uncertainty. This study can be replicated easily for each season and zone within the ISO–NE region.

6.1.2 Clustering According to Weather

We cluster the weather information using the K-means method. As illustrated in Fig. 2, for each additional cluster beyond three, the distortion decreases by less than one. There are no clear ways of choosing the best number of clusters. For this case, three is chosen as the best because it results in acceptable transformed bivariate normality goodness of fit as illustrated in Table 1 whereas using four clusters does not. Fig. 3 compares the original and the clustered weather data for winter, where the three segments labeled 0, 1 and 2 represent the coldest, merely cold and moderate winter days, respectively.

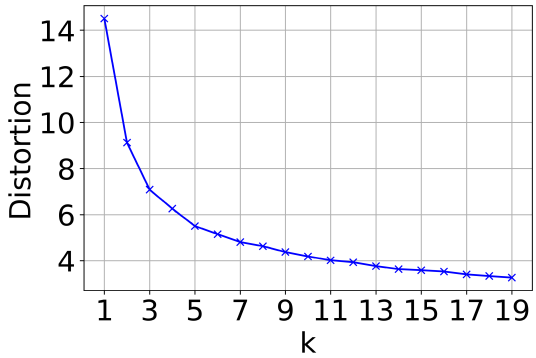

Fig. 2: Clustering optimization distortion of the K-means method

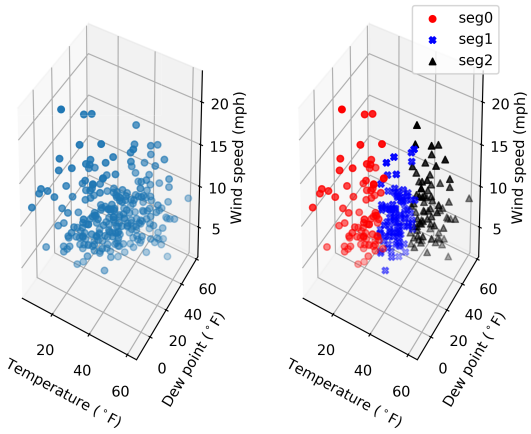

Fig. 3: Winter weather data for CT (a) original; (b) clustered

6.1.3 Joint Distribution of Electric Load and Gas Price

Fig. 4 displays scatterplots of the natural gas price and electric load for each segment of the winter season. The coldest days tend to combine high natural gas price and high electric load, while the moderate days in the winter have relatively low values for both quantities. Table 1 illustrates the results of bivariate normality tests for each segment of winter. Segments 0 and 1 pass all the bivariate normality tests while Segment 2 passes more than half of the tests. The column of result indicates if the dataset follows a normality (i.e., YES or NO) at a significance level of 0.05. Figs. 5–7 show the test results using Q-Q plots, from which we can make two observations. The first is that the histograms of the marginal distributions are approximately bell-shaped and the corresponding univariate Q-Q plots fall close to straight lines, both indicating normality of the marginal distributions. The second observation, from panels (c), is that the bivariate Q-Q plots are nearly linear for most data points except several points at the top right. The Adjusted Mahalanobis distance metric indicates that none of these points are outliers. In addition, a similar process has been followed using the bivariate gamma distribution and the

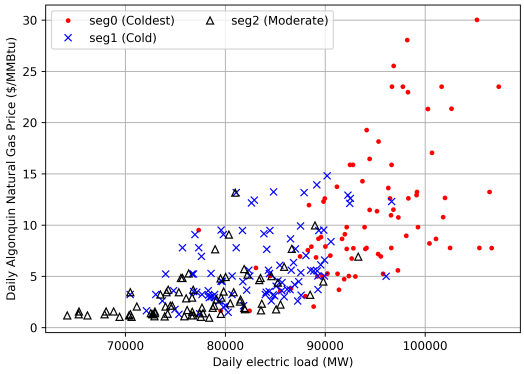

Fig. 4: Winter daily Algonquin price vs. load in CT

statistical results suggest that the bivariate normal distribution performs better [8]. Thus, we selected the bivariate normal distribution to represent the joint uncertainty of daily electric load and natural gas price. In future research, other theoretical or empirical bivariate distributions can also be tested. After obtaining the maximum-likelihood estimate of τ, $y^{(\tau)}$ can be back-transformed to the original scale of observations. The corresponding results as well as the relevant statistical values are listed in Table 2. The coldest segment has the highest expected load and gas price, while the moderate days have the lowest expected load and gas price. Also, each cluster has a different correlation between the transformed load and price.

Table 1: Bivariate normal distribution test results for each segment of the winter season in CT at the 0.05 significance level

	Segment 0			Segment 1			Segment 2		
Test	Test Statistic	p-value	Result	Test Statistic	p-value	Result	Test Statistic	p-value	Result
Univariate Normality									
Shapiro-Wilk									
Load$^{(\tau_1)}$	0.990	0.735	YES	0.989	0.635	YES	0.995	0.988	YES
Price$^{(\tau_2)}$	0.982	0.290	YES	0.976	0.079	YES	0.956	0.009	NO
Bivariate Normality									
Mardia									
Skewness	1.117	0.892	YES	1.474	0.831	YES	0.244	0.993	YES
Kurtosis	0.466	0.641	YES	-1.756	0.079	YES	-2.101	0.036	NO
Henze-zirkler	0.381	0.825	YES	-1.756	0.059	YES	0.778	0.129	YES
Royston	1.228	0.544	YES	3.331	0.191	YES	6.811	0.033	NO
E-statistic	0.547	0.744	YES	0.875	0.111	YES	0.769	0.211	YES

Table 2: Box-Cox transformation maximum-likelihood estimate and bivariate normal fit results for each segment of winter in CT

	τ		Means					
Cluster	Load	Price	Transformed Load (MWh)	Transformed Price ($/MMBtu)	Load (MWh)	Price ($/MMBtu)	Transformed Covariance Matrix	Transformed Correlation
0 (Coldest)	1.019	0.096	115,408	2.501	94,253	9.415	$\begin{bmatrix} 5.364\times10^{7} & 2.956\times10^{3} \\ 2.956\times10^{3} & 5.187\times10^{-1} \end{bmatrix}$	0.560
1 (Cold)	0.682	0.048	3,486	1.700	89,501	5.128	$\begin{bmatrix} 2.588\times10^{4} & 5.017\times10^{1} \\ 5.017\times10^{1} & 4.055\times10^{-1} \end{bmatrix}$	0.490
2 (Moderate)	0.797	-0.464	9,845	0.667	77,388	2.212	$\begin{bmatrix} 3.732\times10^{5} & 1.490\times10^{2} \\ 1.490\times10^{2} & 1.658\times10^{-1} \end{bmatrix}$	0.599

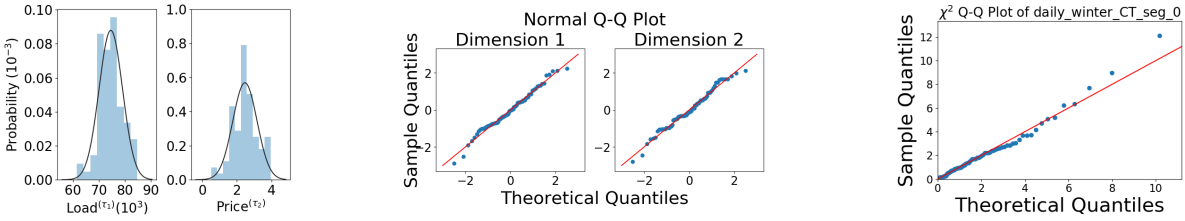

(a) Univariate histogram (b) Univariate Q-Q plot (c) Bivariate Q-Q plot

Fig. 5: Bivariate normal distribution validation for winter segment 0 in CT

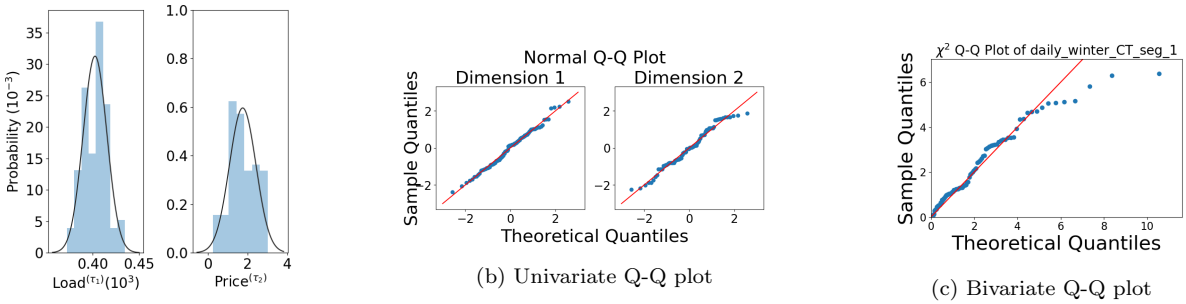

(a) Univariate histogram (b) Univariate Q-Q plot (c) Bivariate Q-Q plot

Fig. 6: Bivariate normal distribution validation for winter segment 1 in CT

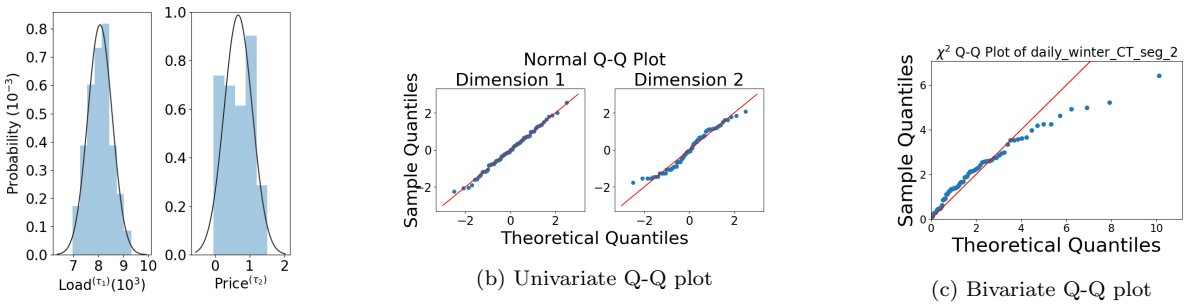

(a) Univariate histogram (b) Univariate Q-Q plot (c) Bivariate Q-Q plot

Fig. 7: Bivariate normal distribution validation for winter segment 2 in CT

6.1.4 Discrete Scenarios Generation

We randomly sample 100,000 observations from the fitted bivariate normal distributions for each segment. Each run of the ED model takes about 3 seconds. For each observation, we have 11 gas availability factors, and thus, simulating ED with 100,000 observations will take approximately 920 hours. We instead use fewer discrete scenarios to represent the uncertainty characteristics of the bivariate normal distribution. We select 30^2 discrete scenarios as described in Section 3. More accurate and tractable scenario generation and reduction methods can be found in [5].

6.2 Effect of Natural Gas Price Uncertainty in Base Case

The case studies are done for each segment of winter because past electricity price spikes have been experienced in cold weather events. To demonstrate the influence of the contracted gas availability on

the simulation results, we use $\rho\overline{G}_{j,t}$ to represent various levels of contracted gas availability by increasing ρ from 0.5 to 1.5 by increments of 0.1. Fig. 8 summarizes the center and spread (mean +/− standard error) of costs from the ED-PE simulation and the ED-PD simulation for each winter segment. For each segment, both the mean and the standard deviation of the total cost from ED-PD simulation are greater than those from the ED-PE simulation, as a result of gas price uncertainty. Specifically, the cost of winter segment 0 (coldest days) has the maximum standard deviation and mean. As the contracted gas availability factor increases, the mean total cost from each simulation first decreases and then becomes stable, illustrating that low contracted gas availability increases the effect of the gas price uncertainty. This happens because given low contracted gas availability, the committed natural gas generator is not able to acquire enough gas from contracts and must acquire gas from the spot market with a possibly high price.

However, the error bars cannot quantify the difference between the ED-PE simulation and the ED-PD simulation. In Fig. 9, bars colored black illustrate the WD measure comparison for various contracted gas availability ρ of each segment. When ρ is less than 1.0, as ρ increases from 0.5 to 1.0, the WD of each segment decreases dramatically. When ρ is greater or equal to 1.0, the WD remains stable. When the actual available gas quantity is less than the nominal value, the dispatch cost experiences high uncertainty due to the uncertain gas price. The CVaR difference between the ED-PD simulation and the ED-PE simulation, indicating the risks coming from gas price uncertainty, shows a pattern of change similar to WD (see Fig. 10). Segment 0 (coldest days) has the largest WD and CVaR difference, compared with segments 1 and 2, indicating the gas price uncertainty has the most impact on dispatch cost distribution risk in the coldest days.

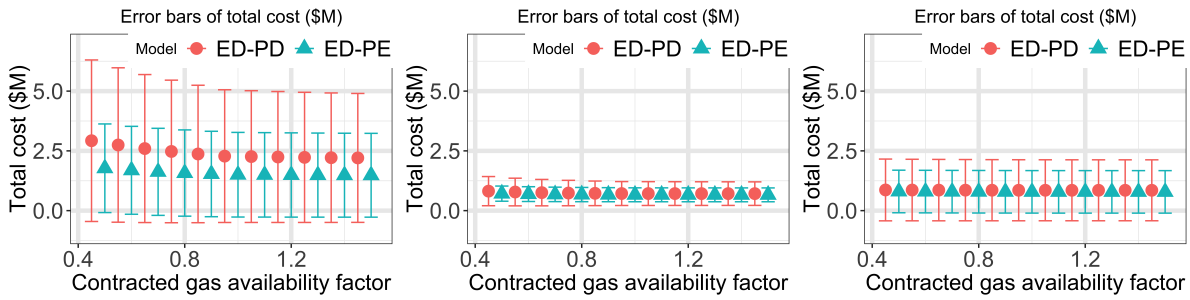

(a) Segment 0 (b) Segment 1 (c) Segment 2

Fig. 8: Error bars of the total cost for each segment of winter in CT

6.3 Comparison of Risk-Mitigation Strategies

We compare the two risk-mitigation strategies of dual fuel conversion and adding a gas storage facility. The idea here is to compare the WD and CVaR difference metrics while applying different risk-mitigation strategies given a fixed investment cost. The strategy that reduces the WD or CVaR difference more dominates the other one. Here we use a simple example to demonstrate the comparison process.

The general dual fuel conversion cost is approximately \$7,500 – \$16,000/MW [1]. We assume the dual conversion cost is \$10,000/MW and totals \$3.15 million for the selected generator. The production cost of using the alternative fuel is \$26.91/MWh. The Inner City Fund expects that it takes \$30 million to construct a storage facility with a capacity of 1.1 Bcf in New England [6]. In addition, we set the cost of filling storage facility as \$2.5/kcf. Then the cost of constructing and filling a new storage facility is $\frac{\$30 \times 10^6}{1.1 \times 10^6 \text{kcf}} + \$2.5/\text{kcf} = \$29.77/\text{kcf}$. Thus the \$3.15 million could alternatively be used to construct and fill one storage facility with capacity $\frac{\$3.15 \times 10^6}{\$29.77/\text{kcf}} = 105,811\text{kcf}$. The hourly maximum outflow is 2,500 kcf [6]. This new storage facility is added at gas node 2 (as strategy 1), where alternatively the connected gas fuel generator is converted to dual fuel in strategy 2. The storage outflow cost is set to be the same as storage facility 1 which is located at gas node 2 as well.

Fig. 9 compares the WD measures while applying various strategies for each segment, displaying the difference between the cost distributions of the ED-PD simulation and the ED-PE simulation. Compared

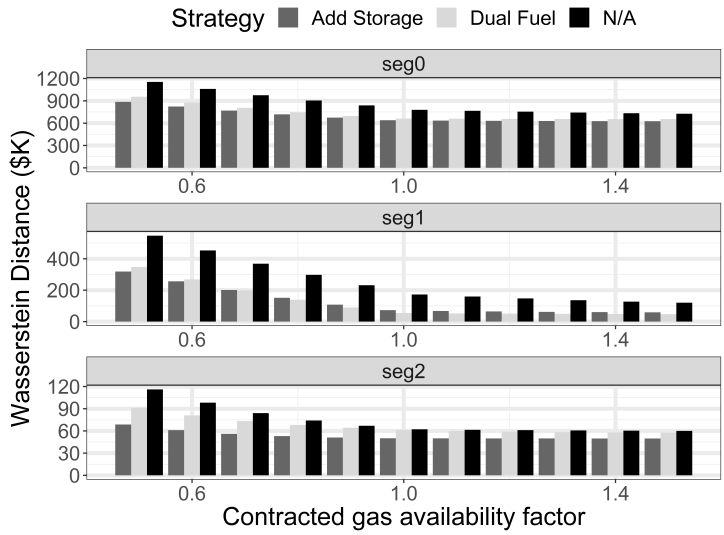

Fig. 9: Wasserstein distance comparison between applying expansion strategies of adding storage, dual fuel conversion and N/A (no strategy applied) for each segment of winter season

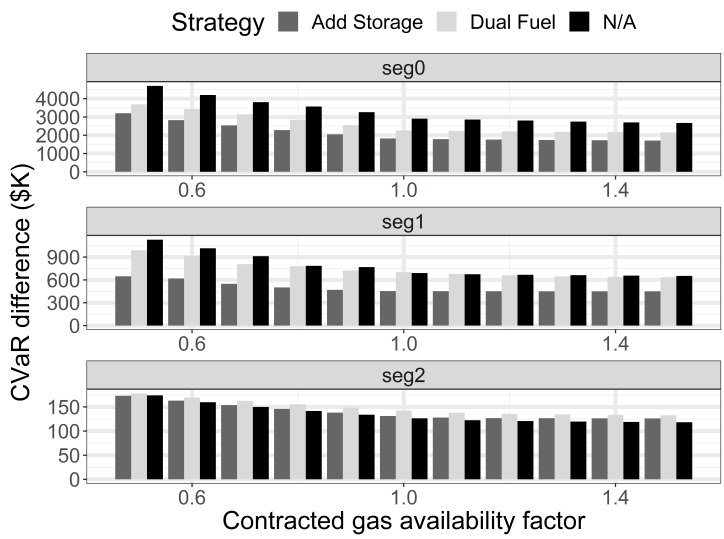

Fig. 10: Conditional value at risk difference due to gas price uncertainty comparison between applying strategies of adding storage, dual fuel conversion and N/A (no strategy applied) for each segment of winter season

with the status quo, either adding storage or converting to dual fuel capability always results in a smaller WD metric, indicating that the effect of gas price uncertainty on the dispatch cost decreases. Moreover, adding the storage facility always results in a smaller WD metric than dual fuel conversion for a fixed investment cost. That is, using WD in the risk measure defined in Section 5.3, we find $\mathrm{WD}^1 \leq \mathrm{WD}^2$. From the WD metric aspect, which indicates the effect of natural gas price uncertainty on the dispatch cost uncertainty, adding a storage facility dominates the dual fuel conversion strategy.

Fig. 10 compares the CVaR difference between the ED-PD and ED-PE simulation which indicates the CVaR risk coming from the gas price uncertainty. For segments 0 and 1, adding either a storage facility or dual fuel capability results in a smaller CVaR difference than no strategy, while for segment 2 both these two strategies result in a larger CVaR difference. This anomaly occurs mainly because we incorporate the risk-mitigation strategies in the unit commitment optimization also and, thus, the inputs of the dispatch problem differ between strategies. Thus, in the moderate days (segment 2), the risk-mitigation strategies do not guarantee reducing the risks coming from natural gas price uncertainty. The risk-mitigation strategies have the most effect on the coldest days, as we can see in Fig. 10 that the CVaR difference for segment 0 is the largest compared with segments 1 and 2. The effect of the risk-

mitigation strategies on the CVaR difference decreases as the contracted gas availability factor increases. In other words, as expected, given less available natural gas from pipelines, the effects of risk-mitigation strategies are more obvious. Specifically, taking the risk measure defined in Section 5.3, the ISO can choose the corresponding values for parameters b_ρ and a_c according to its preference. Here we choose $b_\rho = 1/11$ for each ρ and $a_c = 1/3$ for each c; i.e., we equally weight each value of the gas availability factor and each segment of days. The result is that $\Delta\text{CVaR}_\gamma^0 = \$1.4$ million, $\Delta\text{CVaR}_\gamma^1 = \$0.9$ million, and $\Delta\text{CVaR}_\gamma^2 = \$1.2$ million, where 0, 1, 2 indicate N/A (no strategy applied), adding storage facilities and dual fuel conversion, respectively.

We can also estimate the value of b_ρ using historical data. Here, from 2015-01-01 to 2016-12-31, we find 75, 75 and 61 days in segment 0, 1, and 2 of the winter season, respectively. Hence we can approximate $a_0 = a_1 = 0.36$ and $a_2 = 0.28$. As shown in Table 3, we examined two more cases of $a_c = [0.2, 0.2, 0.6]$ and $a_c = [0.05, 0.05, 0.9]$, where the first one indicates a moderately warm winter and the second one represents a very warm winter. Also, we tested two cases of b_ρ. The first one has $b_\rho = 1/11, \forall\rho$, and the second one sets $b_\rho = [0.025, 0.025, 0.05, 0.10, 0.15, 0.3, 0.15, 0.10, 0.05, 0.025, 0.025]$, which approximates a bell shape. Table 3 compares the CVaR difference for various strategies for different combinations of parameters a_c and b_ρ. We observe that in all the cases, adding storage dominates dual fuel conversion and the status quo since it has the least CVaR difference. In conclusion, given a fixed investment cost, for a winter similar to the historical data or a very warm winter, the storage facility strategy performs best at reducing the risk coming from natural gas price uncertainty. Other combinations of values for b_ρ and a_c can be substituted according to the estimated likelihood and severity of gas constraints and the decision-makers assessment of the relative importance of different segments.

Table 3: CVaR difference comparison among various strategies given different combinations of weight parameters

a_c	b_ρ	CVaR difference ($M)		
		$\Delta\text{CVaR}_\gamma^0$ N/A	$\Delta\text{CVaR}_\gamma^1$ Add Storage	$\Delta\text{CVaR}_\gamma^2$ Dual Fuel
[0.36, 0.36, 0.28]	[1/11, 1/11, 1/11, 1/11, 1/11, 1/11, 1/11, 1/11, 1/11]	1.50	0.99	1.25
	[0.025, 0.025, 0.05, 0.10, 0.15, 0.3, 0.15, 0.10, 0.05, 0.025, 0.025]	1.42	0.92	1.18
[0.20, 0.20, 0.60]	[1/11, 1/11, 1/11, 1/11, 1/11, 1/11, 1/11, 1/11, 1/11]	0.90	0.61	0.76
	[0.025, 0.025, 0.05, 0.10, 0.15, 0.3, 0.15, 0.10, 0.05, 0.025, 0.025]	0.85	0.57	0.72
[0.05, 0.05, 0.90]	[1/11, 1/11, 1/11, 1/11, 1/11, 1/11, 1/11, 1/11, 1/11]	0.33	0.26	0.30
	[0.025, 0.025, 0.05, 0.10, 0.15, 0.3, 0.15, 0.10, 0.05, 0.025, 0.025]	0.31	0.24	0.29

7 Conclusion

In this paper, we proposed a daily economic dispatch model with natural gas from spot market and contracts while considering the natural gas availability constraints and gas fuel cost. Data are clustered based on weather information and, within each cluster, a bivariate normal joint distribution of daily electric load and gas spot market price is estimated by transforming the data, using maximum likelihood estimation to identify a parameter for the transformation. To quantify the effect of uncertain gas spot price on dispatch cost, two cost probability distributions are obtained by simulation. The first one fixes the gas spot price at its point estimate, while the second one incorporates the estimated gas spot price probability distributions. The results for different days clustered according to weather information in winter show that the effect of gas spot price uncertainty is weakened as the contracted gas availability increases. Based on the investment cost and risk reduction comparison, this quantification method can be applied to help choose the most effective risk-mitigation strategy for a given investment cost. Our case study suggests that adding a gas storage facility is preferred over dual fuel conversion. However, since the results are based on an artificial test case, this conclusion is not universal. A system operator could conduct its own case study based on its available data in order to select a better strategy according to the risk metrics.

In future work, this study could be extended to generate probability distributions of the hourly, rather than daily, electric load and spot gas price, and a regression model that relates hourly electric load and

spot gas price to a function of weather data could also be investigated. These extensions require hourly gas price data, which so far we have been unable to obtain. Using discrete scenarios to indicate different levels of contracted gas availability and repeating solving the ED problem with various parameter values is a straightforward way to assess the cost distribution, but either a larger scenario set or a larger test system results in longer computation time. Developing more efficient methods to find the cost distribution given different parameters is necessary. Lastly, how to select the number of discrete scenarios to represent the uncertainty pattern of the transformed bivariate normal distribution could also be investigated in the future.

Acknowledgment

This material is based on work supported by the Power Systems Engineering Research Center as Project M-36.

References

1. Adder JM (2016) ISO-New England dual fuel capabilities to limit natural gas and electricity interdependencies. URL https://www.eenews.net/assets/2017/11/21/document_gw_11.pdf
2. Azzalini A, Capitanio A (1999) Statistical applications of the multivariate skew normal distribution. Journal of the Royal Statistical Society: Series B 61(3):579–602
3. Box GEP, Cox DR (1964) An analysis of transformations. Journal of the Royal Statistical Society Series B (Methodological) pp 211–252
4. Correa-Posada CM, Sanchez-Martin P (2015) Integrated power and natural gas model for energy adequacy in short-term operation. IEEE Transactions on Power Systems 30(6):3347–3355, DOI 10.1109/TPWRS.2014.2372013
5. Dupačová J, Gröwe-Kuska N, Römisch W (2003) Scenario reduction in stochastic programming. Mathematical Programming 95(3):493–511
6. Fang H, Ciatto A, Brock F (2016) U.S. natural gas storage capacity and utilization outlook. URL https://www.energy.gov/sites/prod/files/2017/01/f34/U.S.NaturalGasStorageCapacityandUtilizationOutlook_0.pdf
7. Feng Y, Ryan SM (2016) Day-ahead hourly electricity load modeling by functional regression. Applied Energy 170:455–465
8. Filzmoser P, Garrett RG, Reimann C (2005) Multivariate outlier detection in exploration geochemistry. Computers & Geosciences 31(5):579–587
9. Heitsch H, Römisch W (2007) A note on scenario reduction for two-stage stochastic programs. Operations Research Letters 35(6):731–738
10. Hu D, Ryan SM (2017) Quantifying the effect of natural gas price uncertainty on economic dispatch cost uncertainty. In: Proc. IEEE Power Energy Society General Meeting, pp 1–5, DOI 10.1109/PESGM.2017.8274496
11. Hu D, Ryan SM (2018) Short-term scheduling of a combined natural gas and power system with uncertain wind energy URL http://works.bepress.com/sarah_m_ryan/98/
12. ISO-NE (2016) ISO-NE energy, load and demand reports zonal information. URL https://www.iso-ne.com/isoexpress/web/reports/load-and-demand/-/tree/zone-info
13. Jin J, Kim J (2015) Forecasting natural gas prices using wavelets, time series, and artificial neural networks. PloS One 10(11):e0142064, DOI https://doi.org/10.1371/journal.pone.0142064
14. Klein JB (1998) The use of heat rates in production cost modeling and market modeling. URL http://www.energy.ca.gov/papers/98-04-07_HEATRATE.PDF
15. Korkmaz S, Goksuluk D, Zararsiz G (2014) MVN: An R package for assessing multivariate normalit. The R Journal 6/2, URL https://cran.r-project.org/web/packages/MVN/vignettes/MVN.pdf
16. Li Y, Liu W, Shahidehpour M, Wen F, Wang K, Huang Y (2018) Optimal operation strategy for integrated natural gas generating unit and power-to-gas conversion facilities. IEEE Transactions on Sustainable Energy 9(4):1870 – 1879
17. Midcontinent Independent System Operator (2012) Business practices manual: energy and operating reserve markets. URL https://www.misoenergy.org/legal/business-practice-manuals/
18. Power Systems Control and Automation Laboratory, Georgia Tech Unversity (2018) Three-phase, breaker-oriented IEEE 24-substation reliability test system. URL http://pscal.ece.gatech.edu/archive/testsys/generators.html

19. Rachev ST, Rüschendorf L (1998) Mass Transportation Problems. Volume I: Theory. Springer Science & Business Media
20. Rockafellar RT, Uryasev S (2002) Conditional value-at-risk for general loss distributions. Journal of Banking & Finance 26(7):1443–1471
21. Ryan SM, Gross G, Hu D, Abrantes AL (2018) Analysis of power system operational risks from gas system dependence. URL https://pserc.wisc.edu/publications/reports/2018_reports/M-36_Final_Report.pdf
22. Sugar CA, James GM (2003) Finding the number of clusters in a dataset: an information-theoretic approach. Journal of the American Statistical Association 98(463):750–763
23. The North American Electric Reliability Corporation (2013) Assessment of previous severe winter weather reports 1983-2011. URL https://www.nerc.com/pa/rrm/ea/February%202011%20Southwest%20Cold%20Weather%20Event/Final_Draft_Assessment_of_Previous_Severe_Winter_Weather_Report.pdf
24. The North American Electric Reliability Corporation (2015) 2015 Long-term reliability assessment. URL http://www.nerc.com/pa/RAPA/ra/ReliabilityAssessmentsDL/2015LTRA-FinalReport.pdf
25. US Energy Information Administration (2018) Daily Henry Hub natural gas spot price. URL http://www.eia.gov/dnav/ng/hist/rngwhhdD.htm
26. Yu J, Guo L, Ma M, Kamel S, Li W, Song X (2018) Risk assessment of integrated electrical, natural gas and district heating systems considering solar thermal CHP plants and electric boilers. International Journal of Electrical Power & Energy Systems 103:277–287
27. Zhao B, Conejo AJ, Sioshansi R (2017) Unit commitment under gas-supply uncertainty and gas-price variability. IEEE Transactions on Power Systems 32(3):2394–2405, DOI 10.1109/TPWRS.2016.2602659